Heliyon 10 (2024) e37345

Contents lists available at ScienceDirect

Heliyon

journal homepage: www.cell.com/heliyon

Research article

Radiomic features based on pyradiomics predict CD276 expression associated with breast cancer prognosis

Yong Li [a,b,*], Chun-mei Chen [a,1], Wei-wen Li [a], Ming-tao Shao [a], Yan Dong [a], Qun-chen Zhang [a]

[a] Department of Breast, Jiangmen Central Hospital, Jiangmen City, Guangdong Province, PR China
[b] Department of General Surgery, The First Affiliated Hospital of Jinan University, Guangzhou, Guangdong Province, PR China

ARTICLE INFO

Keywords:
CD276
Magnetic resonance imaging
Radiomics
Prognosis
Breast cancer

ABSTRACT

Background: CD276 is a promising immune checkpoint molecule with significant therapeutic potential. Several clinical trials are currently investigating CD276-targeted therapies.
Purpose: This study aims to assess the prognostic significance of CD276 expression levels and to predict its expression using a radiomic approach in breast cancer (BC).
Methods: A cohort of 840 patients diagnosed with BC from The Cancer Genome Atlas was included in this study. The Cancer Imaging Archive provided 98 magnetic resonance imaging (MRI) scans, which were randomly allocated to training and validation datasets in a 7:3 ratio. The association between CD276 expression and patient survival was assessed using Cox regression analysis. Feature selection was performed using the maximum relevance minimum redundancy algorithm and recursive feature elimination. Subsequently, support vector machine (SVM) and logistic regression (LR) models were constructed to predict CD276 expression.
Results: The expression of CD276 was found to be elevated in BC. It was an independent risk factor for overall survival (hazard ratio = 1.579, 95 % CI: 1.054–2.366). There were eight radiomic features selected in total. In both the training and validation subsets, the SVM and LR models demonstrated favorable predictive abilities with AUC values of 0.744 and 0.740 for the SVM model and 0.742 and 0.735 for the LR model. These results indicate that the radiomic models efficiently differentiate the CD276 expression status.
Conclusions: CD276 expression levels can have an impact on cancer prognosis. The MRI-based radiomic signature described in this study can discriminate the CD276 expression status.

1. Introduction

Breast cancer represents a significant malignancy affecting women worldwide, constituting the second most common cause of cancer-related mortality [1]. Presently, the primary therapeutic approaches for breast cancer include surgical intervention, radiotherapy, and chemotherapy. Survival rates exhibit considerable regional disparities, with developed countries reporting an estimated

* Corresponding author. Department of Breast, Jiangmen Central Hospital, No. 23, Haibang St., Beijie, Jiangmen City, Guangdong Province, 529030, PR China.
E-mail addresses: docleo1985@sina.com (Y. Li), chchmei1989@163.com (C.-m. Chen), 271482038@qq.com (W.-w. Li), sdbxsmt@163.com (M.-t. Shao), m13437322874@163.com (Y. Dong), qczhang2014@163.com (Q.-c. Zhang).
[1] Co-first author.

https://doi.org/10.1016/j.heliyon.2024.e37345
Received 15 February 2024; Received in revised form 30 August 2024; Accepted 2 September 2024
Available online 3 September 2024

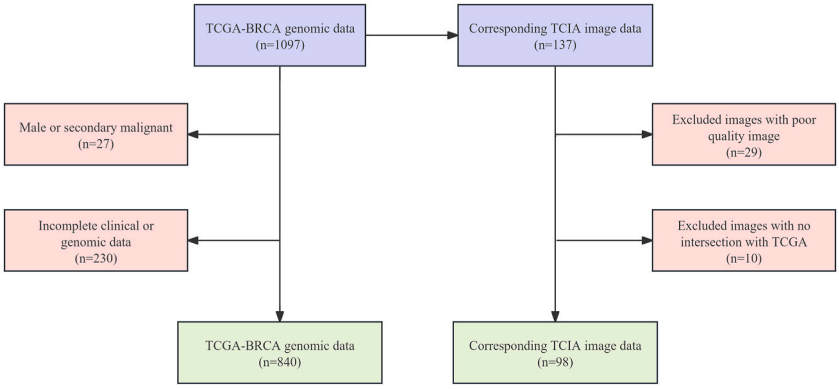

Fig. 1. Flowchart of the data collection and analysis. (TCIA: The Cancer Imaging Archive, TCGA: stands for The Cancer Genome Atlas Program.)

5-year survival rate of approximately 80 %, in contrast to less than 40 % in developing countries. In clinical practice, mammography and magnetic resonance imaging (MRI) serve as the principal diagnostic techniques for detecting breast cancer.

The traditional prognostic factors for breast cancer, which include clinicopathological characteristics and biomarkers such as carcinoembryonic antigen (CEA), human epidermal growth factor receptor 2 (HER-2), and cancer antigen 153 (CA153), are insufficient to meet the demands of precision medicine in clinical practice. Consequently, there is a pressing need to investigate novel prognostic markers and devise patient stratification methodologies to enable individualized treatment. This approach holds promise for advancing personalized precision therapy.

Anti–PD-1/PD-L1 has received significant attention, and it exhibited good therapeutic effect in the triple-negative breast cancer [2]. CD276 (B7-H3) is markedly expressed in breast cancer tissues, and its overexpression correlates with decreased disease severity, lower risk of recurrence, and improved survival rates. Analogous to the extensively studied B7-H1 (PD-L1), CD276 belongs to the B7 family of proteins. It represents a promising target for cancer immunotherapy and has recently garnered significant attention for its substantial therapeutic potential [3,4]. Numerous studies have reported that in solid tumors, targeted CD276 therapy exhibits antitumor activity and has huge application potential [5–7]. A study reported that CD276 antibody–drug conjugates are highly effective against HER2-negative breast cancers [8]. Several clinical trials targeting CD276 are ongoing [4].

MRI constitutes the principal modality for acquiring image data critical to clinical diagnosis. The incorporation of artificial intelligence into medical imaging is increasingly catalyzing substantial advancements in the field. Radiomics, characterized as a high-throughput image sequencing technique, facilitates the extraction of a multitude of image parameters. This noninvasive and dynamic detection method quantitatively represents tumor characteristics, thereby enhancing diagnostic precision [9]. Previous studies have demonstrated the potential of radiomic technology in facilitating the timely identification and categorization of breast cancer, as well as assessing residual lesions, lymph node burden, tumor heterogeneity, and tumor microenvironment.

Based on the above factors, in this study, we set out to construct a MRI-based radiomic model to predict the expression of CD276 in breast cancer. At the same time, bioinformatic analysis was used to assess the association between CD276 expression and prognosis in breast cancer.

2. Materials and methods

2.1. Patients and datasets

The Cancer Genome Atlas (TCGA) was used to obtain clinicopathological and transcriptomic data, while the Cancer Imaging Archive (TCIA) was used to obtain MRI data. We downloaded and normalized RNA-sequencing (RNA-seq) data from TCGA using the Xiantao tool (https://www.xiantao.love/products). TCGA data were excluded based on the following criteria: male, no survival data, survival time less than 30 days, no clinical data, and no RNA sequencing. Exclusion criteria for TCIA data included tumor resection images and poor quality MRI images. In total, 840 patients from TCGA and 98 patients from TCIA participated in this study. Fig. 1 illustrated a brief flowchart. Ethical approval was not required because this was an analysis of data from public databases.

2.2. Survival analysis based on TCGA cohort

The cohort was first classified into high and low CD276 expression groups using the R package Survminer. To assess the difference in patient survival between high and low CD276 expression groups, a Kaplan-Meier curve and log rank test were used. A multivariate and univariate Cox regression analysis were conducted to identify the independent impact of CD276 expression on overall survival (OS). Finally, an exploratory subgroup analysis was conducted for exploring the effect of CD276 on OS in different patient subgroups.

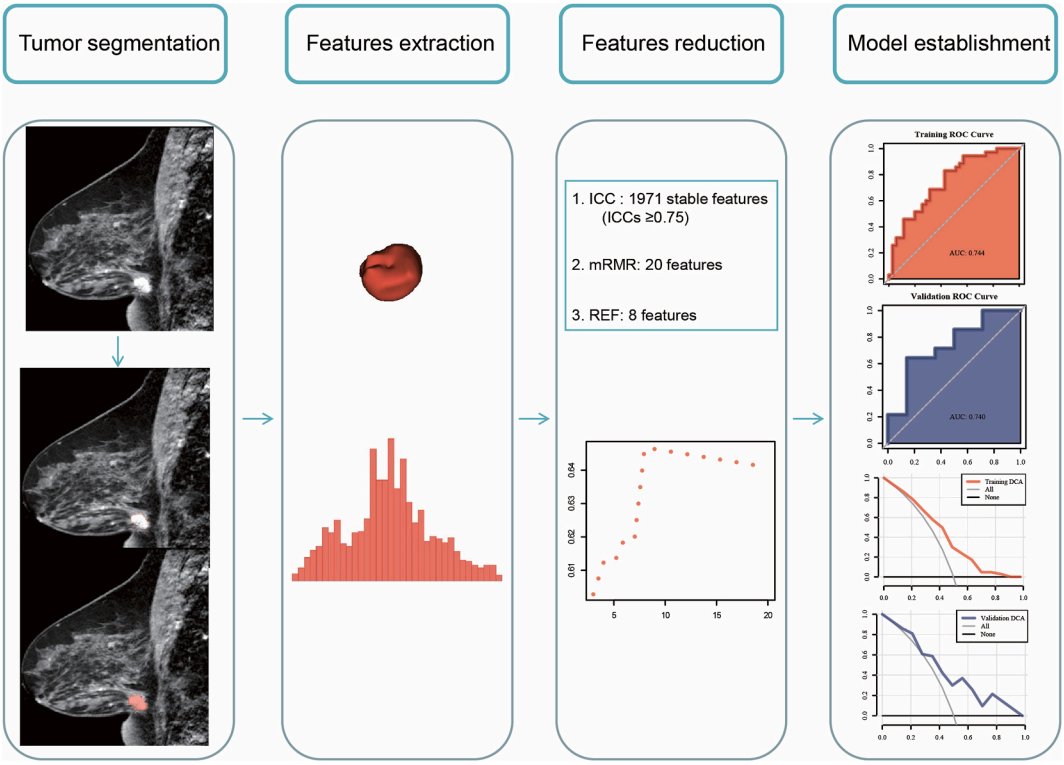

Fig. 2. Brief flowchart of radiomic progression. TCIA, The Cancer Imaging Archive; TCGA, The Cancer Genome Atlas; HCC, hepatocellular carcinoma; mRMR, maximum relevance minimum redundancy algorithm; RFE, recursive feature elimination; ROC, receiver operating characteristic; AUC, area under the curve; DCA, decision curve analysis.

2.3. Comprehensive analysis of functional and immune characteristics based on TCGA

Gene Set Enrichment Analysis (GSEA) was performed using R package clusterProfiler (https://guangchuangyu.github.io/software/clusterProfiler) to identify differentially expressed genes (DEGs) between CD276 high and low expression groups. ImmuCellAI (http://bioinfo.life.hust.edu.cn/web/ImmuCellAI/) was used to obtain and evaluate immune cell infiltration scores of the TCGA cohort. We then extracted immune checkpoint-related genes to screen for differentially expressed immune-checkpoint genes between groups with high and low CD276 expression.

2.4. Segmentation of region of interest and extraction of features from MRI images

A radiomic flowchart is briefly shown in Fig. 2. The 98 patients were randomly divided into training and validation sets in 7:3 ratio. N4ITK algorithm was used to account for the locally varying intensity in MRI. For the analysis of the entire tumor region, we selected the phase of the dynamic contrast-enhanced magnetic resonance imaging (DCE-MRI) that exhibited the most pronounced lesion enhancement. During the delineation process, we conducted a thorough evaluation of both plain and dynamic contrast-enhanced MRI images. By adjusting the window width and window level appropriately, we accurately identified the lesion location. Subsequently, we performed bilateral comparisons to detect any abnormal soft tissue masses, structural changes, signal discrepancies, and areas of abnormal enhancement, thereby ensuring precise delineation of the tumor region. A manual segmentation of the volume of interest (VOI) was performed using the 3D Slicer software (version 4.10.2). The images were evaluated by a senior radiologist unaware of the patient's clinical information. To verify the robustness of the radiomic features, images of 30 cases were randomly chosen to delineate lesions and extract radiomic features.

2.5. Selection of radiomic features

Radiomic features were extracted using PyRadiomics (https://github.com/Radiomics/pyradiomics). There were 2060 radiomic features, including 93 original, 14 shape, 744 texture, 465 log [sigma = (1.0, 2.0, 3.0, 4.0, 5.0)], 93 square, 93 squareroot, 93 exponential, 93 logarithm, 279 lbp, and 93 gradient features. Two radiologists independently delineated the volumes of interest (VOIs) for the purpose of extracting radiomic features. Upon completion of delineation for all cases by the first radiologist, a random sample of 30 cases was selected using a random number table for delineation and feature extraction by the second radiologist. The intraclass

Table 1
Clinical characteristics of patients with breast cancer from TCGA.

Variables	Total (n = 840)	Low (n = 438)	High (n = 402)	*P*
Age, n (%)				<0.001
< 60	465 (55)	218 (50)	247 (61)	
≥60	375 (45)	220 (50)	155 (39)	
M_stage, n (%)				0.064
M0	697 (83)	374 (85)	323 (80)	
M1/MX	143 (17)	64 (15)	79 (20)	
N_stage, n (%)				0.016
N0	382 (45)	217 (50)	165 (41)	
N1/N2/N3/NX	458 (55)	221 (50)	237 (59)	
T_stage, n (%)				0.239
T1	229 (27)	130 (30)	99 (25)	
T2	480 (57)	244 (56)	236 (59)	
T3/T4	131 (16)	64 (15)	67 (17)	
ER_status, n (%)				0.45
Negative	190 (23)	94 (21)	96 (24)	
Positive	650 (77)	344 (79)	306 (76)	
PR_status, n (%)				0.631
Negative	268 (32)	136 (31)	132 (33)	
Positive	572 (68)	302 (69)	270 (67)	
HER2_status, n (%)				0.207
Negative	439 (52)	234 (53)	205 (51)	
Positive	131 (16)	59 (13)	72 (18)	
Unknown	270 (32)	145 (33)	125 (31)	
Histological_type, n (%)				0.501
Infiltrating Ductal Carcinoma	655 (78)	337 (77)	318 (79)	
Infiltrating Lobular Carcinoma	185 (22)	101 (23)	84 (21)	
Margin_status, n (%)				0.768
Negative	711 (85)	367 (84)	344 (86)	
Positive/Close	86 (10)	47 (11)	39 (10)	
Unknown	43 (5)	24 (5)	19 (5)	
Radiotherapy, n (%)				0.082
No	393 (47)	218 (50)	175 (44)	
Yes	447 (53)	220 (50)	227 (56)	
Chemotherapy, n (%)				0.146
No	355 (42)	196 (45)	159 (40)	
Yes	485 (58)	242 (55)	243 (60)	

correlation coefficient (ICC) values were subsequently calculated utilizing the 'irr' package in R. The ICC values were interpreted according to standard thresholds: values of ≥0.75 indicate excellent agreement, values between 0.51 and 0.74 indicate moderate agreement, and values below 0.50 indicate poor agreement. The features with ICC >0.75 were selected for further analysis. The top-20 features were extracted by the Maximum relevance and minimum redundancy (mRMR) method, and the optimal subset of features was selected using recursive feature elimination (RFE).

2.6. Construction and evaluation of radiomic models

Support vector machine (SVM) and logistic regression (LR) were used to construct the respective prediction models. Furthermore, receiver operating characteristic (ROC) analyses were conducted to determine the area under the curve (AUC). The calibration curve and Brier score were used to evaluate the model calibration degree. We assessed the model goodness-of-fit with the Hosmer-Lemeshow tests. A decision curve analysis (DCA) was conducted to evaluate its clinical efficacy. The radiomic score (RS) represents the predictive probability of the model. A Wilcoxon rank-sum test was used to compare RS between groups with high and low CD276 expression. The AUC values of the two models were compared using the Delong test.

2.7. Statistical analysis

Student *t*-test, Pearson's correlation analysis, and Wilcoxon rank-sum test were performed as appropriate. The data used in this study were analyzed using SPSS 23.0 (IBM SPSS, SPSS Inc.) and R packages (version 4.0.3). Cox proportional hazard models were used to calculate hazard ratios (HRs) with 95 % confidence intervals (CI). Data were analyzed using R statistical software packages. The two-sided significance level was set at 0.05.

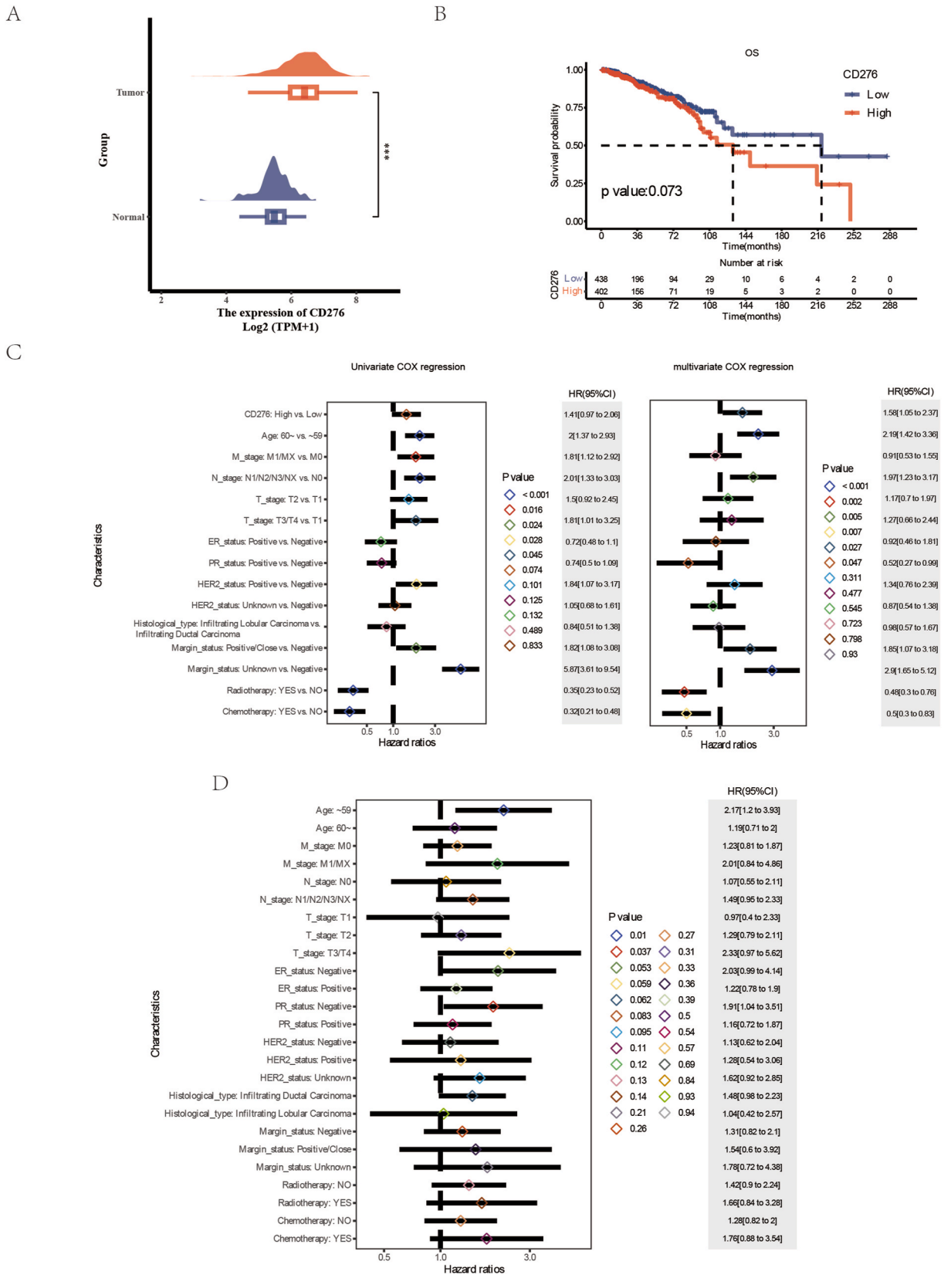

(caption on next page)

Fig. 3. Comparison of clinical and survival data. (A) Higher CD276 expression was observed in cancer samples compared with normal tissues. (B) Kaplan-Meier curves of OS in patients with high/low CD276 expression levels. (C) Univariate and multivariate analyses for HCC patients. (D) Subgroup analysis and interaction test for the prognostic value of CF276. (*: $p < 0.05$; **: $p < 0.01$; ***: $p < 0.001$).

3. Results

3.1. Baseline characteristics of patients

A cohort of 840 breast cancer patients was stratified into low (n = 438) and high (n = 402) CD276 expression groups based on a cutoff value of 4.712 for subsequent analyses. The baseline characteristics of these groups are detailed in Table 1. High CD276 expression was significantly associated with younger age (P = 0.001) and a more advanced N stage (P = 0.016). No significant differences were observed between the groups regarding histology, T stage, M stage, ER, PR, HER2 status, margin status, radiotherapy, or chemotherapy (P > 0.05). The Wilcoxon rank-sum test indicated that CD276 levels were significantly higher in breast cancer than in normal controls (P < 0.001) (Fig. 3A).

3.2. Survival analysis and Cox regression analysis

The median survival times for the low and high CD276 expression groups were 219.8 and 131.4 months, respectively. The Kaplan–Meier curve demonstrated an association between elevated CD276 expression and reduced overall survival (OS) (P = 0.073) (Fig. 3B). Univariate analysis identified high CD276 expression as a risk factor for OS (hazard ratio [HR] = 1.412, 95 % confidence interval [CI] = 0.967–2.062, P = 0.074) (Fig. 3C). Multivariate analysis further confirmed CD276 expression as an independent risk factor for OS (HR = 1.579, 95 % CI = 1.054–2.366, P = 0.027) (Fig. 3C). Subgroup analyses indicated no significant interactions among the subgroups (Fig. 3D).

3.3. Biological function of CD276 in breast cancer

The 40 most significantly enriched KEGG pathways identified through GSEA are illustrated in Fig. 4A. Within the KEGG gene sets, differentially expressed genes (DEGs) were notably enriched in the pathways associated with cancer. The hallmark gene sets demonstrated significant enrichment in epithelial-mesenchymal transition, TNFA signaling via NF-κB, and oxidative phosphorylation, as depicted in Fig. 4B. Analysis of immune infiltrations indicated a significant increase in the infiltration of CD4 T cells and NKT cells, whereas a significant decrease was observed in CD8 T cell infiltration within the high CD276 expression group (P < 0.001) (Fig. 4C). Analysis of immune checkpoint expression revealed the expression of immune checkpoint genes to be mostly higher among high CD276 expression groups than among low CD276 expression groups ($P < 0.05$) (Fig. 4D).

3.4. Extraction of radiomic features

A mean ICC value of 0.978 was achieved for the radiomic features. A total of 1,971 radiomic features with an ICC value greater than 0.75 were selected. Subsequently, the top 20 features were identified using the Minimum Redundancy Maximum Relevance (mRMR) method. Ultimately, the eight most optimal features were selected through RFE.

3.5. Establishment and evaluation of radiomic model

No statistically significant differences in demographic and clinical characteristics were observed between the high and low CD276 expression groups in both the training and validation sets (Tables 2 and 3).

Two machine learning classifiers, namely, SVM and LR, were used to establish the radiomic models. ROC curves for the performance of the two models in the training and validation cohorts were shown in Figs. 5 and 6.

The importance of the selected features in the SVM algorithm was shown in Fig. 5A. The SVM model exhibited satisfactory predictive ability with an AUC of 0.744 and 0.740 in the training and validation cohorts, respectively (Fig. 5 B and 5C). Additionally, the Brier scores for the training and validation cohorts were 0.218 and 0.221, respectively.

In a similar manner, the importance of the selected features in the LR algorithm was shown in Fig. 6A. The LR model achieved AUC values of 0.742 and 0.735 in the training and validation cohorts, respectively (Fig. 6B and C). The Brier scores for the training and validation cohorts were 0.202 and 0.205, respectively. The Hosmer–Lemeshow goodness-of-fit tests indicated no evidence of poor calibration in either model (Fig. 5D and E; Fig. 6D and E). Additionally, DCA plots demonstrated high clinical validity for both prediction models (Fig. 5F and G; Fig. 6F and G).

The RS differed significantly in both training cohorts ($P < 0.001$) (Fig. 5H) and validation cohorts ($P < 0.05$) (Fig. 5I) for the SVM model, with higher RS values in the high CD276 expression cohort.

In LR model, RS significantly varied between the two CD276 expression groups in the training cohort ($P < 0.01$) (Fig. 6H) and validation cohort ($P < 0.05$) (Fig. 6I), also with increased RS values in the high CD276 expression group.

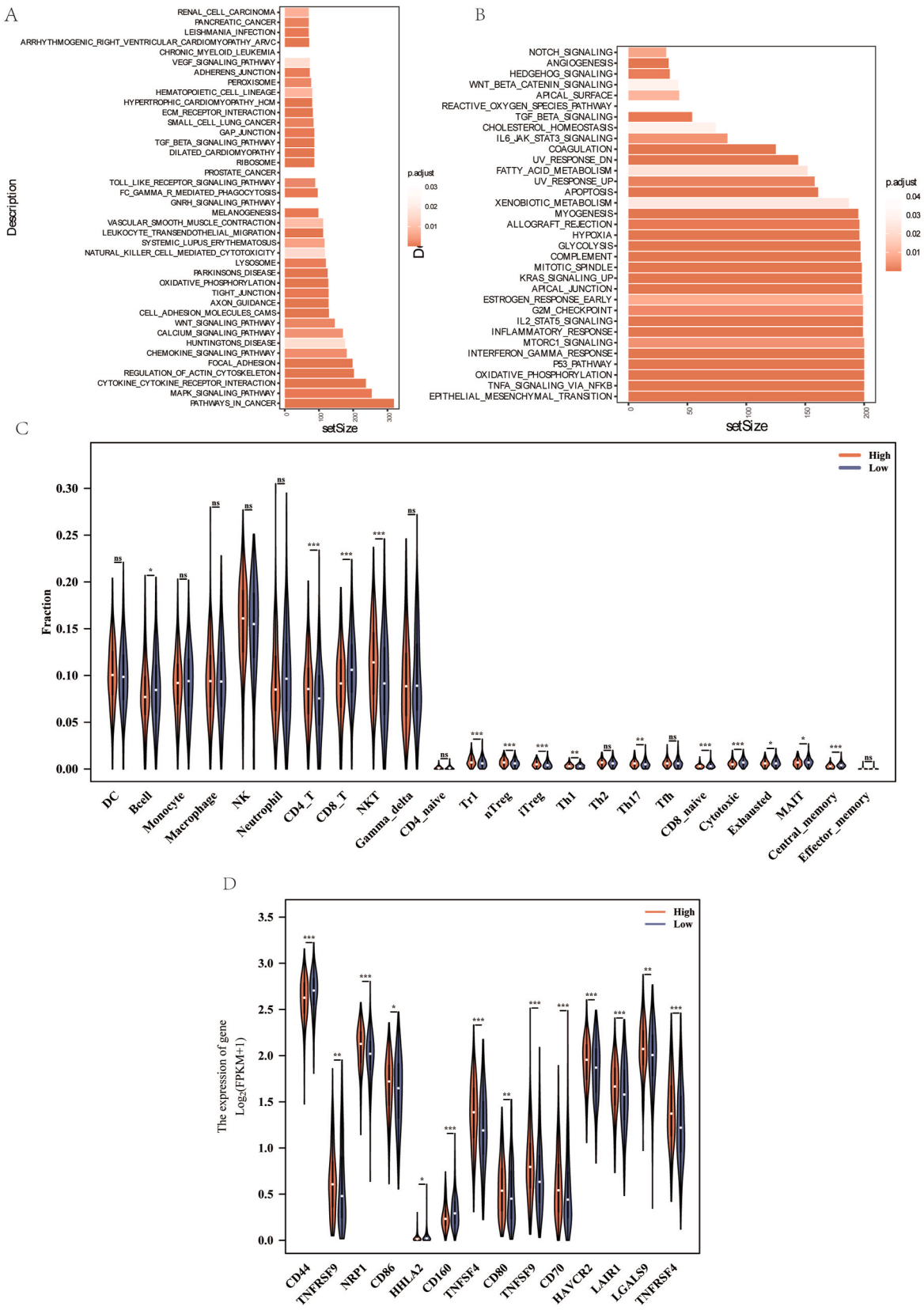

(caption on next page)

Fig. 4. Biological analysis of differentially expressed genes between the high and low groups. (A) GSEA analysis based on the KEGG gene set. (B) GSEA analysis based on the Hallmark gene set. (C) Immune cell infiltration analysis. (D) Immune checkpoint expression analysis. (*: $p < 0.05$; **: $p < 0.01$; ***: $p < 0.001$).

Table 2
Demographic and clinical characteristics of the training dataset.

Variables	Total (n = 70)	Low (n = 35)	High (n = 35)	*P*
Age, n (%)				0.805
< 60	44 (63)	23 (66)	21 (60)	
≥60	26 (37)	12 (34)	14 (40)	
M_stage, n (%)				1
M0	66 (94)	33 (94)	33 (94)	
M1/MX	4 (6)	2 (6)	2 (6)	
N_stage, n (%)				1
N0	33 (47)	16 (46)	17 (49)	
N1/N2/N3/NX	37 (53)	19 (54)	18 (51)	
T_stage, n (%)				0.652
T1	25 (36)	12 (34)	13 (37)	
T2	43 (61)	21 (60)	22 (63)	
T3/T4	2 (3)	2 (6)	0 (0)	
ER_status, n (%)				0.733
Negative	10 (14)	6 (17)	4 (11)	
Positive	60 (86)	29 (83)	31 (89)	
PR_status, n (%)				0.765
Negative	14 (20)	8 (23)	6 (17)	
Positive	56 (80)	27 (77)	29 (83)	
HER2_status, n (%)				0.741
Negative	40 (57)	20 (57)	20 (57)	
Positive	8 (11)	3 (9)	5 (14)	
Unknown	22 (31)	12 (34)	10 (29)	
Histological_type, n (%)				0.733
Infiltrating Ductal Carcinoma	60 (86)	29 (83)	31 (89)	
Infiltrating Lobular Carcinoma	10 (14)	6 (17)	4 (11)	
Margin_status, n (%)				0.28
Negative	62 (89)	30 (86)	32 (91)	
Positive/Close	5 (7)	2 (6)	3 (9)	
Unknown	3 (4)	3 (9)	0 (0)	
Radiotherapy, n (%)				0.427
No	20 (29)	12 (34)	8 (23)	
Yes	50 (71)	23 (66)	27 (77)	
Chemotherapy, n (%)				1
No	16 (23)	8 (23)	8 (23)	
Yes	54 (77)	27 (77)	27 (77)	
Survival status, n (%)				1
Alive	69 (99)	34 (97)	35 (100)	
Dead	1 (1)	1 (3)	0 (0)	

3.6. AUC comparisons in different prediction models

DeLong's test was used to compare the ROC curve of both models. In terms of the AUC values, no significant difference was observed between the training and validation cohorts of the SVM model ($P = 0.973$) and the LR model ($P = 0.948$). In the training and validation sets, the AUC values of SVM and LR models were similar ($P = 0.917$ and 0.902, respectively). Both models demonstrated good fit and exhibited a high degree of reliability.

4. Discussion

In this study, patients with breast cancer who presented with higher CD276 expression were observed to have worse prognosis. The expression of CD276 was linked with young age and lymph node metastases. Further analyses were carried out to understand the biological significance of CD276 expression in breast cancer. In addition, MRI-based radiomic models were developed and validated to evaluate CD276 expression preoperatively. Based on our results, we found that higher RS was associated with higher CD276 expression. This radiomic model predicting CD276 expression would assist doctors in making more accurate clinical decisions.

CD276 is overexpressed in solid tumors, which was correlated with poor prognosis [10,11]. A significant increase in CD276 expression was observed in cancer tissues compared to normal tissues in our study. CD276 was found to be an independent prognostic factor for OS in multivariate analysis. According to a meta-analysis, high CD276 expression is associated with later TNM stage and shorter overall survival [12].

Table 3
Demographic and clinical characteristics of the validation dataset.

Variables	Total (n = 28)	Low (n = 14)	High (n = 14)	*P*
Age, n (%)				0.385
< 60	21 (75)	9 (64)	12 (86)	
≥60	7 (25)	5 (36)	2 (14)	
M_stage, n (%)				1
M0	25 (89)	13 (93)	12 (86)	
M1/MX	3 (11)	1 (7)	2 (14)	
N_stage, n (%)				1
N0	15 (54)	7 (50)	8 (57)	
N1/N2/N3/NX	13 (46)	7 (50)	6 (43)	
T_stage, n (%)				0.185
T1	13 (46)	9 (64)	4 (29)	
T2	12 (43)	4 (29)	8 (57)	
T3/T4	3 (11)	1 (7)	2 (14)	
ER_status, n (%)				1
Negative	6 (21)	3 (21)	3 (21)	
Positive	22 (79)	11 (79)	11 (79)	
PR_status, n (%)				1
Negative	9 (32)	4 (29)	5 (36)	
Positive	19 (68)	10 (71)	9 (64)	
HER2_status, n (%)				1
Negative	15 (54)	7 (50)	8 (57)	
Positive	5 (18)	3 (21)	2 (14)	
Unknown	8 (29)	4 (29)	4 (29)	
Histological_type, n (%)				1
Infiltrating Ductal Carcinoma	27 (96)	13 (93)	14 (100)	
Infiltrating Lobular Carcinoma	1 (4)	1 (7)	0 (0)	
Margin_status, n (%)				1
Negative	27 (96)	14 (100)	13 (93)	
Unknown	1 (4)	0 (0)	1 (7)	
Radiotherapy, n (%)				1
No	9 (32)	4 (29)	5 (36)	
Yes	19 (68)	10 (71)	9 (64)	
Chemotherapy, n (%)				1
No	7 (25)	4 (29)	3 (21)	
Yes	21 (75)	10 (71)	11 (79)	
Survival status, n (%)				1
Alive	28 (100)	14 (100)	14 (100)	

To gain insights into the biological basis for the poor prognosis, DEGs between high and low CD276 expression groups were analyzed. GSEA analysis indicated that the KEGG pathways-in-cancer, KEGG MAPK-signaling-pathway, hallmark epithelial-mesenchymal-transition, and hallmark TNFA-signaling-via-NF-κB were highly enriched in the high CD276 expression group. The pathways-in-cancer involved diverse signaling pathways, such as the MAPK, p53, and PI3K-Akt signaling pathways. These pathways can influence cancer initiation and progression [13]. Epithelial–mesenchymal transition is crucial to cancer metastasis. High CD276 expression and CD8_T infiltration were negatively correlated in immune infiltration analysis. CD276 exerts an inhibitory immune effect by preventing activation of $CD8^+$ T-lymphocytes [14]. In addition, co-deficiency of CD276 and B7-H4 is correlated to better prognosis and increased infiltration of $CD8^+$ T-cells [15]. Our study found that the high CD276 expression group exhibited high levels of immune checkpoints. High expression of immune checkpoints leads to inefficient antitumor immunity, which was prone to the development of immunosuppressive microenvironment to promote tumor immune escape [16,17]. These findings provided insights regarding the novel functions of CD276 in breast cancer development. The mechanisms underlying these effects should be comprehensively investigated in future studies.

Radiomics is an effective and noninvasive method for the prediction of gene expression status. In recent years, studies on radiomics to predict PD-L1 expression in tumor have gradually increased [18–21]. Until now, this is the first study to use a quantitative radiomic mode to predict CD276 expression status. We found that both our radiomic models performed well on the training and validation sets, with AUCs of 0.744 for the SVM model and 0.742 for the LR model. These two models had good discriminatory ability and accuracy in the training and validation sets. According to our study, MRI radiomics can be used to predict CD276 expression accurately. Our radiomic models incorporated higher-order detailed features. The prediction model was constructed using eight radiomic features, of which five were wavelet features. The wavelet transform increased the information of low-frequency signal, amplified the subtle intensity variation between regions, and represented the intensity inhomogeneity within a region, which cannot be detected with naked eye [22,23]. Wavelet-transformed textures exhibited better performance in predicting the pathological complete response for breast cancer than volumetric and/or peripheral textures [24,25].

This study has some limitations. First, this study was retrospective with a small sample size; prospective external validation with a larger sample size will be necessary in the future. Second, the data were obtained from public databases, and our results may be influenced by the quality of data. Third, only mRNA level, and not protein expression, of CD276 was analyzed.

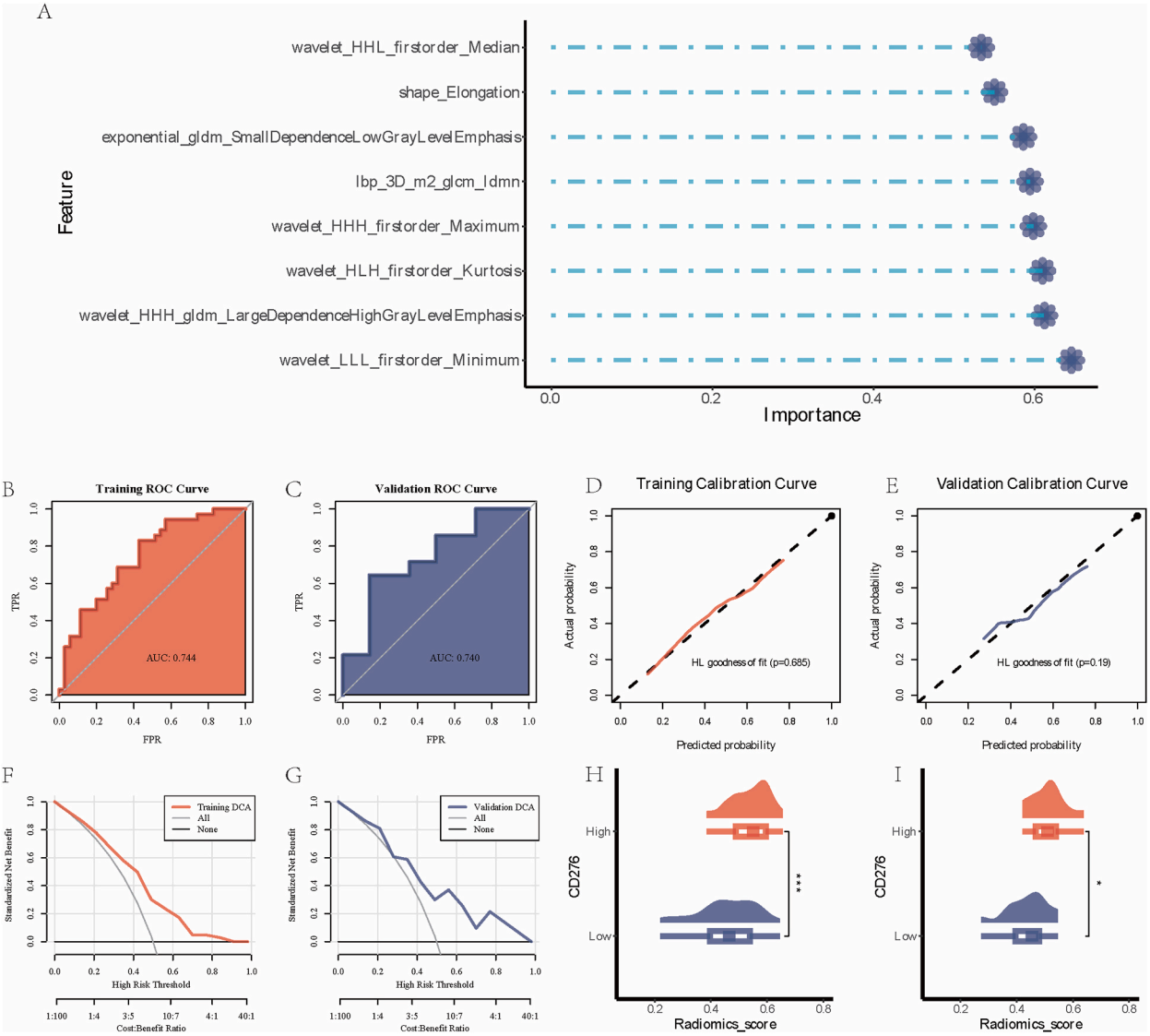

Fig. 5. Evaluation of the SVM model. (A) The weights of the selected radiomics features. (B, C) ROC curves of model in the training and validation cohorts. (D, E) Calibration curves of model in the training and validation cohorts. (F, G) DCAs of model in the training and validation cohorts. (H, I) The difference in radiomics score in the training and validation cohorts.

In conclusion, the expression levels of CD276 can significantly influence the prognosis of patients with breast cancer. Based on MR images, the radiomic features can effectively predict the expression level of CD276.

Institutional review board statement

The study was conducted in accordance with the Declaration of Helsinki and abides by the TCIA Data Usage Policy; all datasets were de-identified, thus did not require institutional review board approval.

Informed consent statement

Patient informed consent was waived due to the retrospective nature of this study.

Data availability statement

Publicly available datasets were analyzed in this study. This data can be found in: TCGA (portal.gdc.cancer.gov); and TCIA (https://tcia.at/home).

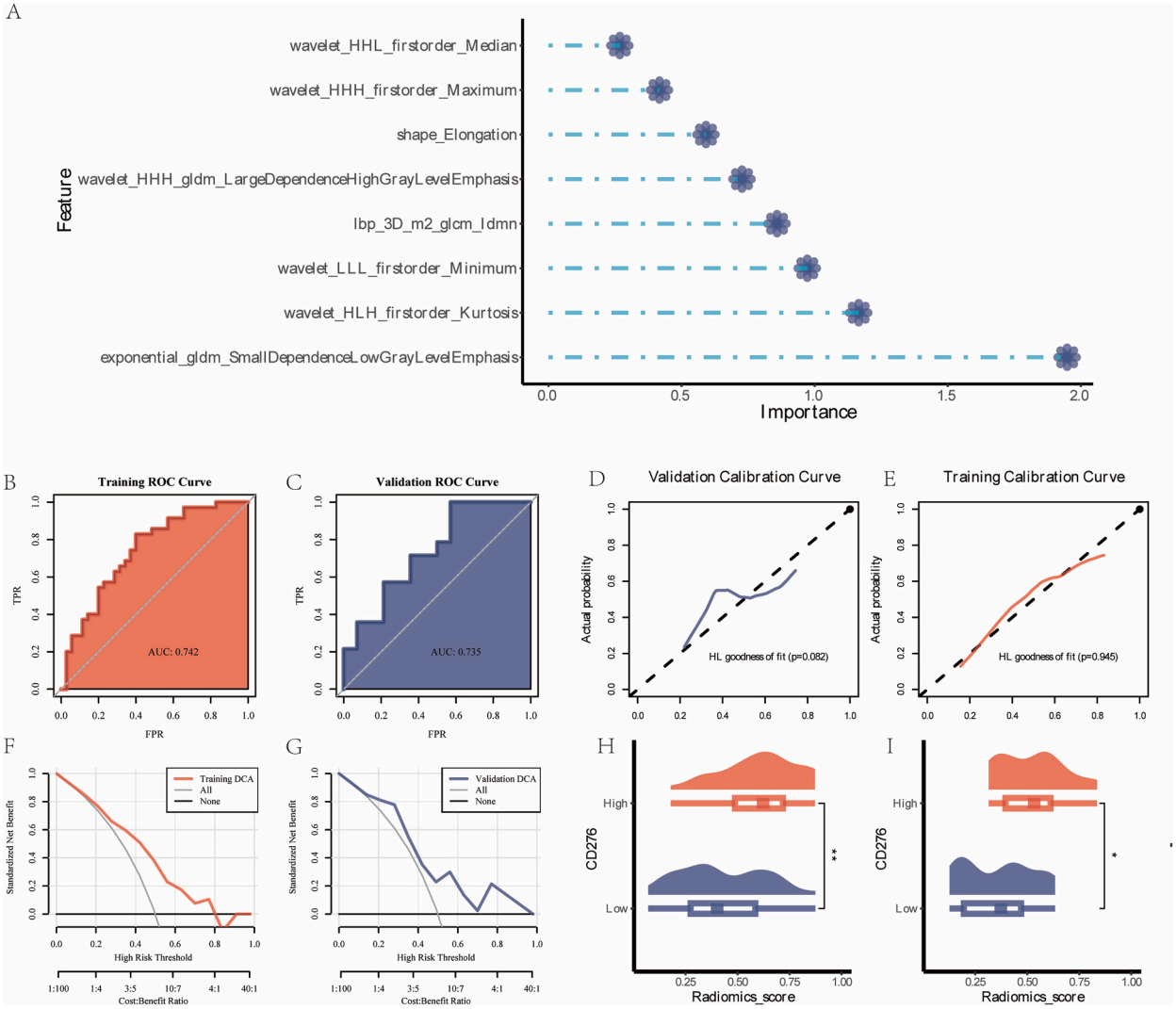

Fig. 6. Evaluation of the LR model. (A) The weights of the selected radiomics features. (B, C) ROC curves of model in the training and validation cohorts. (D, E) Calibration curves of model in the training and validation cohorts. (F, G) DCAs of model in the training and validation cohorts. (H, I) The difference in radiomics score in the training and validation cohorts.

CRediT authorship contribution statement

Yong Li: Writing – review & editing, Writing – original draft, Visualization, Validation, Supervision, Conceptualization. **Chun-mei Chen:** Writing – review & editing, Writing – original draft, Methodology, Investigation. **Wei-wen Li:** Writing – original draft, Validation, Conceptualization. **Ming-tao Shao:** Writing – original draft, Investigation, Data curation. **Yan Dong:** Writing – original draft, Software. **Qun-chen Zhang:** Writing – original draft, Validation.

Declaration of competing interest

The authors declare that they have no known competing financial interests or personal relationships that could have appeared to influence the work reported in this paper.

References

[1] C. Fitzmaurice, T.F. Akinyemiju, F.H. Al Lami, et al., Global, regional, and national cancer incidence, mortality, years of life lost, years lived with disability, and disability-adjusted life-years for 29 cancer groups, 1990 to 2016: a systematic analysis for the global burden of disease study, JAMA Oncol. 4 (11) (2018) 1553–1568.

[2] S. Kumar, M. Chatterjee, P. Ghosh, K.K. Ganguly, M. Basu, M.K. Ghosh, Targeting PD-1/PD-L1 in cancer immunotherapy: an effective strategy for treatment of triple-negative breast cancer (TNBC) patients, Genes Dis 10 (4) (2023) 1318–1350.

[3] X. Huang, J. Guo, S. Wang, et al., Global research trends on B7-H3 for cancer immunotherapy: a bibliometric analysis (2012-2022), Hum. Vaccines Immunother. 19 (2) (2023) 2246498.
[4] B. Zhao, H. Li, Y. Xia, et al., Immune checkpoint of B7-H3 in cancer: from immunology to clinical immunotherapy, J. Hematol. Oncol. 15 (1) (2022) 153.
[5] J.A. Scribner, J.G. Brown, T. Son, et al., Preclinical development of MGC018, a duocarmycin-based antibody-drug conjugate targeting B7-H3 for solid cancer, Mol. Cancer Therapeut. 19 (11) (2020) 2235–2244.
[6] X. Zhang, H. Guo, J. Chen, et al., Highly proliferative and hypodifferentiated CAR-T cells targeting B7-H3 enhance antitumor activity against ovarian and triple-negative breast cancers, Cancer Lett. 572 (2023) 216355.
[7] S.H. Shin, E.J. Ju, J. Park, et al., ITC-6102RO, a novel B7-H3 antibody-drug conjugate, exhibits potent therapeutic effects against B7-H3 expressing solid tumors, Cancer Cell Int. 23 (1) (2023) 172.
[8] Y. Feng, J. Lee, L. Yang, et al., Engineering CD276/B7-H3-targeted antibody-drug conjugates with enhanced cancer-eradicating capability, Cell Rep. 42 (12) (2023) 113503.
[9] L. Gao, W. Jiang, Q. Yue, et al., Radiomic model to predict the expression of PD-1 and overall survival of patients with ovarian cancer, Int. Immunopharm. 113 (Pt A) (2022) 109335.
[10] O. Melaiu, V. Lucarini, R. Giovannoni, D. Fruci, F. Gemignani, News on immune checkpoint inhibitors as immunotherapy strategies in adult and pediatric solid tumors, Semin. Cancer Biol. 79 (2022) 18–43.
[11] X. Lei, Z. Ou, Z. Yang, et al., A pan-histone deacetylase inhibitor enhances the antitumor activity of B7-H3-specific CAR T cells in solid tumors, Clin. Cancer Res. 27 (13) (2021) 3757–3771.
[12] H. Su, X. Lin, J. Huo, F. Zhang, Clinicopathological features and prognostic value of CD276 expression in breast cancer: a meta-analysis, Asian J. Surg. 46 (11) (2023) 5323–5329.
[13] Y. Dai, W. Qiang, X. Yu, et al., Guizhi Fuling Decoction inhibiting the PI3K and MAPK pathways in breast cancer cells revealed by HTS(2) technology and systems pharmacology, Comput. Struct. Biotechnol. J. 18 (2020) 1121–1136.
[14] J. Leitner, C. Klauser, W.F. Pickl, et al., B7-H3 is a potent inhibitor of human T-cell activation: No evidence for B7-H3 and TREML2 interaction, Eur. J. Immunol. 39 (7) (2009) 1754–1764.
[15] S. Si, L. Wang, H. Cao, Y. Xu, Q. Zhan, Co-deficiency of B7-H3 and B7-H4 identifies high CD8 + T cell infiltration and better prognosis in pancreatic cancer, BMC Cancer 22 (1) (2022) 211.
[16] G.P. Dunn, A.T. Bruce, H. Ikeda, L.J. Old, R.D. Schreiber, Cancer immunoediting: from immunosurveillance to tumor escape, Nat. Immunol. 3 (11) (2002) 991–998.
[17] Z. Gong, J. Zhang, W. Guo, Tumor purity as a prognosis and immunotherapy relevant feature in gastric cancer, Cancer Med. 9 (23) (2020) 9052–9063.
[18] X. Zhao, Y. Zhao, J. Zhang, Z. Zhang, L. Liu, X. Zhao, Predicting PD-L1 expression status in patients with non-small cell lung cancer using [(18)F]FDG PET/CT radiomics, EJNMMI Res. 13 (1) (2023) 4.
[19] Y. Cui, Y. Lin, Z. Zhao, H. Long, L. Zheng, X. Lin, Comprehensive (18)F-FDG PET-based radiomics in elevating the pathological response to neoadjuvant immunochemotherapy for resectable stage III non-small-cell lung cancer: a pilot study, Front. Immunol. 13 (2022) 994917.
[20] Gullo R. Lo, H. Wen, J.S. Reiner, et al., Assessing PD-L1 expression status using radiomic features from contrast-enhanced breast MRI in breast cancer patients: initial results, Cancers 13 (24) (2021).
[21] Z. Wu, Q. Lin, H. Wang, et al., Intratumoral and peritumoral radiomics based on preoperative MRI for evaluation of programmed cell death ligand-1 expression in breast cancer, J. Magn. Reson. Imag. 60 (2) (2024) 588–599.
[22] R. Jing, J. Wang, J. Li, et al., A wavelet features derived radiomics nomogram for prediction of malignant and benign early-stage lung nodules, Sci. Rep. 11 (1) (2021) 22330.
[23] W.H. Fang, X.D. Li, H. Zhu, et al., Resectable pancreatic ductal adenocarcinoma: association between preoperative CT texture features and metastatic nodal involvement, Cancer Imag. 20 (1) (2020) 17.
[24] J. Zhou, J. Lu, C. Gao, et al., Predicting the response to neoadjuvant chemotherapy for breast cancer: wavelet transforming radiomics in MRI, BMC Cancer 20 (1) (2020) 100.
[25] L. Guo, S. Du, S. Gao, et al., Delta-radiomics based on dynamic contrast-enhanced MRI predicts pathologic complete response in breast cancer patients treated with neoadjuvant chemotherapy, Cancers 14 (14) (2022).